# Optimized Moving-Average Filtering for Gradient Artefact Correction During Simultaneous EEG-fMRI

José L. Ferreira*, Ronald M. Aarts, and Pierre J.M. Cluitmans

***Abstract*—The strong capability of the combined EEG-fMRI for investigating and revealing new insights on mapping of the brain activity as well as on several other neuroscientific studies has attracted the interest of researchers and clinicians over the past years. However, its consolidation as a powerful and independent technique still depends on enhancing the quality of the EEG signal, mainly due to the occurrence of artefacts. This paper presents a simple and effective approach for removal of the gradient artefact, which is induced in the EEG by the rapidly varying gradient magnetic fields of the fMRI scanner. According to our method, a moving-average filter is used to perform the removal of the gradient artefact. Nevertheless, rather than estimation of an artefact waveform template to be subtracted and achieve the EEG restoration, we have proposed to optimize the moving-average filtering process along the entire EEG excerpt. Thereby, the restored EEG can be estimated either from a sum of partial waveform components resulting from the recursive application of the optimized moving-average filter; or from an estimative of the artefact along the entire excerpt. Our methodology shows to achieve a quite satisfactory restoration of the EEG signal, even for low signal amplitudes. Moreover, in addition to predict the variability of the artefact waveform over the time, synchronization between EEG and fMRI clocks and extensive data segmentation are not required as well.**

***Keywords*—Simultaneous EEG-fMRI; gradient artefact removal; optimized moving-average filtering; signal slope adaption; harmonic artefact filtering.**

## I. Introduction

The advent of the functional magnetic resonance imaging (fMRI) around two decades ago [1] allowed the possibility to combine this technique with electroencephalography (EEG) in neuroscience research and other related studies. Rather than only an additional tool for monitoring the human brain activity, combined EEG-fMRI has revealed to be quite promising and powerful for mapping of the brain activity. Thus, it has been extended to other applications and drawn the attention of several researchers and clinicians in recent years [2].

*J. L. Ferreira is with the Department of Electrical Engineering, Eindhoven University of Technology, P.O. Box 513, Eindhoven, The Netherlands (phone: +31 40 247 4137 – email: j.l.ferreira@tue.nl).

R. M. Aarts is with the Department of Electrical Engineering, Eindhoven University of Technology, P.O. Box 513, Eindhoven, The Netherlands, and also with the Philips Research Eindhoven, The Netherlands (email: r.m.aarts@tue.nl).

Pierre J.M. Cluitmans is with the Department of Electrical Engineering, Eindhoven University of Technology, P.O. Box 513, Eindhoven, The Netherlands, and also with the Kempenhaeghe Epilepsy Center, The Netherlands (email: p.j.m.cluitmans@tue.nl).

Nevertheless, consolidation and enlarging the range of applications of the combined EEG-fMRI still depend on enhancing the quality of the EEG signal acquired simultaneously with the fMRI data. During simultaneous acquisition of the EEG and fMRI, the EEG signal can be corrupted and distorted by three types of artefacts, which are induced by the magnetic fields of the fMRI equipment: (i) the artefact associated with the head subject movements within the scanner; (ii) the pulse or ballistocardiogram artefact, provoked by the pulsatile movement of the blood in scalp arteries within the static magnetic field ($B_0$); and (iii) the gradient or imaging acquisition artefact [3, 4, 5, 6]. Gradient artefacts arise in the EEG signal due to the voltage induced by the application of rapidly varying magnetic field gradients for spatial encoding of the MR signal, and radiofrequency pulses (RF) for spin excitation, in the circuit formed by the electrodes, leads, patient and amplifier [5]. Their amplitudes can be several orders of magnitude (up to $10^4$ μV) higher than the neuronal EEG signal (up to 300 μV) [5, 7]. In case of continuous fMRI acquisition, the bandwidth of the standard clinical EEG is exceeded by high-frequency artefact components, in addition to being overlapped by discrete harmonic artefact frequency intervals, or frequency bins. According to [8], the fundamental of each respective frequency bin corresponds to multiples of the inverse of the echo-planar imaging (EPI) parameter slice time. In turn, for periodic fMRI, i.e., with delays between EPI volumes, harmonics in the frequency range of the volume repetition frequency are convolved with the clinical EEG as well [4, 5].

In the literature, a number of solutions have been proposed to attenuate the effects of gradient artefacts on the EEG signal at the source [5, 9]. Nonetheless, as those methods do not carry out the complete removal of the artefact, post-processing signal solutions have been also proposed and employed for gradient artefact correction and subsequent EEG restoration. In this respect, the average artefact subtraction (AAS) methodology [4] is the most established technique for gradient artefact removal. This approach is based upon the stationary and periodic nature of the artefact, whereby an average artefact waveform is estimated and subtracted from the EEG signal in the regions in which the artefact occurs. However, the performance of the AAS method depends on accurate sampling of the gradient artefact waveform. It requires time-alignment between fMRI scanner and EEG clocks as well [10, 11, 12, 13]. Head motions of the subject within the fMRI scanner can also compromise its efficacy, because of the alterations and transients that are inserted in the artefact waveform, resulting in an inaccurate averaging process [14]. Hence, additional

information associated with the head movements must be quantified and used for obtaining a superior artefact correction [15, 16].

Other gradient artefact correction techniques in the time or frequency-domain have been proposed as well, like sum-of-sinusoidal modelling for artefact waveform estimation [17], principal component analysis [8, 18], independent component analysis [19], spatial filtering [20], and frequency-domain filtering [21, 22, 23]. According to [24], there is no optimal approach for gradient artefact correction, and certain algorithms may be preferred depending on the type of data analysis pursued. Their improvement and the development of further correction methods are even demanded in order to enhance the quality of the EEG correction, mainly regarding EEG signals with low amplitude or high-frequency activity, and under the occurrence of abrupt subject head motions [9, 12, 16, 18]. This paper presents a novel and simple methodology for gradient artefact correction based upon optimized moving-averaging (MA) filtering. According to our method, estimation of the artefact is not performed by an artefact waveform averaging or curve fitting procedure. Rather, we have proposed a recursive forward-backward application of the moving-average filter along the entire EEG excerpt, in such a way that the gradient artefact is optimally estimated, and then subtracted in order to restore the signal. Alternatively, the restored EEG signal can be estimated by a sum of partial components obtained during the iterative application of the MA filter, as described in the section Methods. Combination of the optimized moving-average filter approach with the nonlinear filter proposed by [25] allows obtaining a quite satisfactory EEG restoration during periodic or continuous fMRI. Furthermore, extensive data segmentation as well as time-alignment between EEG and fMRI clocks are not required within the implementation of the proposed approach.

## II. METHODS

### A. Subjects

The EEG recordings were collected simultaneously with the fMRI data for a research focused on epilepsy and post-traumatic stress disorder (PTSD) [17, 26]. All participants were male and aged between 18 and 60 years. EEG recordings from 15 subjects were selected in order to apply and evaluate the methodology proposed in this work.

### B. EEG and fMRI Data

Functional magnetic resonance imaging scanning was carried out using a 3 T Scanner (Philips, Eindhoven, The Netherlands). An MRI-compatible 64 channel polysomnograph (MRI 64, MicroMed, Treviso, Italy) was used to collect one ECG channel, two EOG channels, one EMG channel, and 60 EEG channels. The sampling rate for signal acquisition was 2048 Hz. The subjects were scanned using a functional echo-planar imaging (EPI) sequence with 33 transversal slices (thickness 3 mm, TE 30 ms, TR 2500 ms). EEG electrodes positioning was in accordance with the international 10-20 system electrodes placement [27]. The EEG recordings were acquired during periodic fMRI acquisition.

### C. Proposed Methodology for Gradient Artefact Removal

Our methodology was implemented in accordance with the algorithm block diagram of Fig. 1. Each step of the algorithm was developed and applied to the EEG recordings in MATLAB environment. Equation (1) was taken into account to model the raw EEG signal, $\mathbf{EEG}_{\mathbf{raw}}$:

$$\mathbf{EEG}_{\mathbf{raw}} = \mathbf{EEG}_{\mathbf{true}} + \mathbf{G}_{\mathbf{artf}} + \mathbf{n} \tag{1}$$

where $\mathbf{EEG}_{\mathbf{true}}$ corresponds to the true EEG signal; $\mathbf{G}_{\mathbf{artf}}$ is the gradient artefact; and $\mathbf{n}$ represents the additional noise.

#### 1) Peak detection and ST estimation

Implementation of the methodology illustrated in Fig. 1 requires the initial detection of the typical gradient artefact peaks, which are observed in the raw EEG data recorded within the MR scanner. Such detection is necessary for estimation of the EPI slice time, *ST*, parameter used during implementation of the optimized moving-average filter (step 3 of Fig. 1). In order to detect the peaks, we have used the peak detection algorithms proposed by [28]. For the data under analysis, the value of *ST* was estimated at $155 \pm 1$ samples, which corresponds to the time interval of $75.68 \pm 0.50$ ms [27]. Hence, the slice time was set as $ST = 155$ samples.

#### 2) Nonlinear filtering by signal slope adaption (SSD)

Large signal slopes associated with the gradient artefact can be used to identify and correct artefact components [27]. Based on this idea, the usage of a nonlinear filter approach to improve the restoration of the EEG signal has been proposed in [25] in such a way that residual high-frequency as well as underlying artefact components within the EEG bandwidth could be attenuated. Such a nonlinear filter makes use of the signal slope adaption (SSD) approach [29], whose implementation takes into account probability distributions of the difference between consecutive samples of artefact free EEG excerpts (*diff* ($\mathbf{EEG}_{\mathbf{true}}$)), and EEG excerpts containing gradient artefacts (*diff* ($\mathbf{EEG}_{\mathbf{raw}}$)) [17].


Fig. 1. Block diagram structure of the proposed methodology for gradient artefact correction.

Thereby, the gradient artefact activity can be attenuated by adapting signal slopes of the raw EEG, according to the threshold *thrs* [17, 25]:

$$thrs = \mu_{diff(\mathbf{EEG}_{true})} + 3\sigma_{diff(\mathbf{EEG}_{true})} \quad (2)$$

The nonlinear filter approach by SSD was applied in the step 2 (Fig. 1), as a pre-processing procedure of our methodology, in order to obtain an attenuated artefact ($\mathbf{A}_{artf}$). The resulting signal after attenuation of the gradient artefact constitutes the signal $\mathbf{EEG}_{corct}$:

$$\mathbf{EEG}_{corct} = \mathbf{E\hat{E}G}_{true} + \mathbf{A}_{artf} + \mathbf{n} \quad (3)$$

*3) Optimized moving-average filtering*

A moving-average (MA) filter corresponds to a finite impulse response (FIR) filter, described by (4) [30, 31]:

$$y_i = \sum_{k=0}^{N} c_k x_{i-k} \quad (4)$$

where $x$ and $y$ are, respectively, the input and output signals of the filter; $c_k$ are the filter coefficients or tap weights ($k = 0,1,2,\ldots, N$); and $N$ is the order of the filter. A simple moving-average filter is the Hanning filter, which corresponds to the arithmetic mean of the values of the input signal:

$$y_i = \frac{1}{N}\sum_{k=0}^{N-1} x_{i-k} \quad (5)$$

To remove the gradient artefact from the EEG signal, we have proposed to use an optimized Hanning filter, as follows. The time *ST* between the gradient artefact peaks (slices) was used to set the order of the MA filter, i.e., $N = 155$. Assuming that the gradient artefact waveform is stationary (i.e., it can be considered a slowly varying process) and has zero mean, application of such a moving-average filter to the raw EEG only would run over values associated with the true EEG signal. Hence, the resulting average waveform would correspond to the mean variation of the EEG signal along the entire excerpt. Therefore, assuming that the terms of (3) are uncorrelated, forward-backward application of (5) to the $\mathbf{EEG}_{corct}$ results in the waveform $\mathbf{EEG}_{rest,1}$, which can be characterized as an averaged approximation of the $\mathbf{E\hat{E}G}_{true}$:

$$\mathbf{EEG}_{rest,1} \approx \mathbf{E\hat{E}G}_{true} \quad (6)$$

The MA filter acts as a smoothing low-pass filter, in such a way that the signal $\mathbf{EEG}_{rest,1}$ contains low-frequency activity associated with the $\mathbf{E\hat{E}G}_{true}$. In turn, the frequency activity associated with the gradient artefact is contained in the signal $\mathbf{EEG}_{high,1}$, resulting from the subtraction of the $\mathbf{EEG}_{rest,1}$ from the $\mathbf{EEG}_{corct}$:

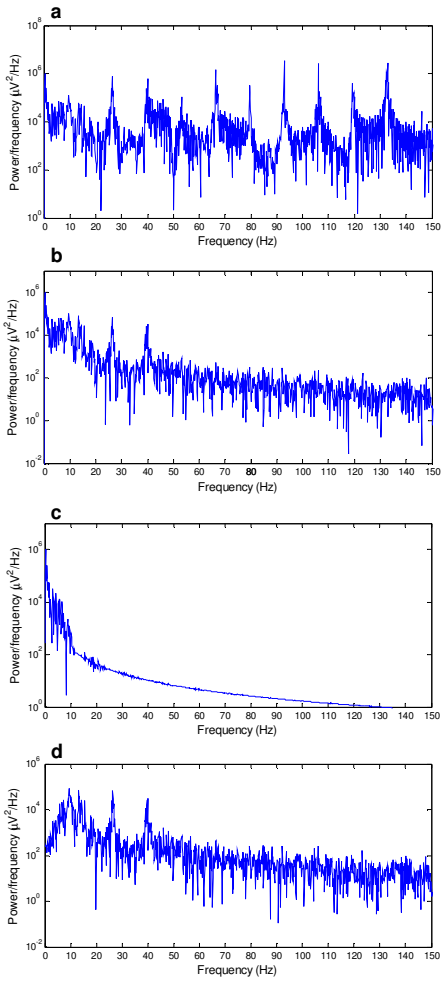


Fig. 2. (a) Power spectrum of the raw EEG signal; (b) power spectrum of the $\mathbf{EEG}_{corct}$; (c) power spectrum of the signal $\mathbf{EEG}_{rest,1}$; (d) power spectrum of the signal $\mathbf{EEG}_{high,1}$. Harmonics of the repetitive slice sequence related to the gradient artefact can be observed at multiples of 13.2 Hz in (a), (b), and (d), but are not contained in (c).

$$\mathbf{EEG}_{high,1} = \mathbf{EEG}_{corct} - \mathbf{EEG}_{rest,1} \quad (7)$$

Those characteristics can be observed in the power spectra depicted in Fig. 2. The power spectra of this figure correspond to the signals $\mathbf{EEG}_{rest,1}$ and $\mathbf{EEG}_{high,1}$, and the associated $\mathbf{EEG}_{raw}$ and $\mathbf{EEG}_{corct}$. Such raw EEG excerpt was extracted from the recordings of one subject, electrode position FP1. Since high-frequency components associated with the $\mathbf{E\hat{E}G}_{true}$ remain in the $\mathbf{EEG}_{high,1}$, we applied (5) in the latter signal again, in order to obtain an estimation of such components. The second forward-backward application of the MA filter, therefore, results in the signal $\mathbf{EEG}_{rest,2}$, and the $\mathbf{EEG}_{high,2}$ can be obtained from the subtraction:

$$\mathbf{EEG}_{high,2} = \mathbf{EEG}_{high,1} - \mathbf{EEG}_{rest,2} \quad (8)$$

This procedure was repeated so forth, until a number $J$ of iterations had been reached. Therefore, the recursive application of the MA filter allows that the remaining partial components $\mathbf{EEG_{rest,\mathit{j}}}$, of the $\mathbf{E\hat{E}G_{true}}$, are estimated and separated from the signal $\mathbf{EEG_{high,\mathit{j}}}$. Thus, at each iteration, the amplitude (or the maximum magnitude) of the $\mathbf{EEG_{rest,\mathit{j}}}$ tends to approximate to 0. In other words, increasing the number of iterations, $j \rightarrow J$, the $\mathbf{EEG_{high,\mathit{j}}}$ can be optimally approximated to the gradient artefact, $\mathbf{A_{artf}}$:

$$\lim_{\max\left|\mathbf{EEG}_{\mathbf{rest},j}\right|\rightarrow 0} \mathbf{EEG}_{\mathbf{high},J} = \mathbf{A}_{\mathbf{artf}} \tag{9}$$

In this case limit, therefore, the restored EEG ($\mathbf{E\hat{E}G_{true}}$) corresponds to either the subtraction between the $\mathbf{EEG_{corct}}$ and $\mathbf{EEG_{high,\mathit{J}}}$:

$$\mathbf{E\hat{E}G}_{\mathbf{true}} = \mathbf{EEG}_{\mathbf{corct}} - \mathbf{EEG}_{\mathbf{high},J} \tag{10}$$

or the sum of the partial waveform components resulting from the recursive application of the optimized MA filter:

$$\mathbf{E\hat{E}G}_{\mathbf{true}} = \sum_{j=1}^{J} \mathbf{EEG}_{\mathbf{rest},j} \tag{11}$$

*4) Consistency analysis*

A set of EEG validation channels, FP1, F3, F8, T5, P3, Oz, CP1, FC5, AFz, F6, C2, TP7, CP4, and POz, was used for evaluation of the proposed gradient artefact correction approach. For validation purposes, we have compared the power spectra of EEG excerpts recorded in the fMRI scanner with and without fMRI, as performed by [4]. The power spectrum was calculated for the range of the clinical EEG (0 – 24 Hz) [4, 17, 25]. A comparison between the signal restorations obtained by our methodology and by the AAS method was also made.

## III. RESULTS

Fig. 3 depicts the application of the methodology proposed in this work. The raw EEG signal (Fig. 3a) and the $\mathbf{EEG_{corct}}$ (Fig. 3b) are the same ones whose power spectra are shown in Fig. 2. The raw EEG signal depicted in Fig. 3a contains artefact interference at 1.4mV pk-pk, whereas after application of the nonlinear filter such interference was attenuated to 25.8 µV pk-pk (Fig. 3b). The respective restored EEG is shown in Fig 3c, for a number $J = 200$ iterations of the MA filter. In Fig. 4, the power spectrum of the $\mathbf{EEG_{corct}}$ is also depicted, jointly with the power spectrum of the restored EEG. It can be noticed that the optimized MA filter attenuates the frequency components at the artefact frequency bins (multiples of 13.2 Hz). This characteristic is observed in the approximated flat regions of the spectrum of Fig. 4b. As the EEG data were recorded during periodic fMRI, the delay time ($DT$) between consecutive volumes occurred in the raw EEG signal of Fig. 3a, at 160.35, 162.85, and 165.35 s. The volume repetition frequencies components associated with the $DT$ were

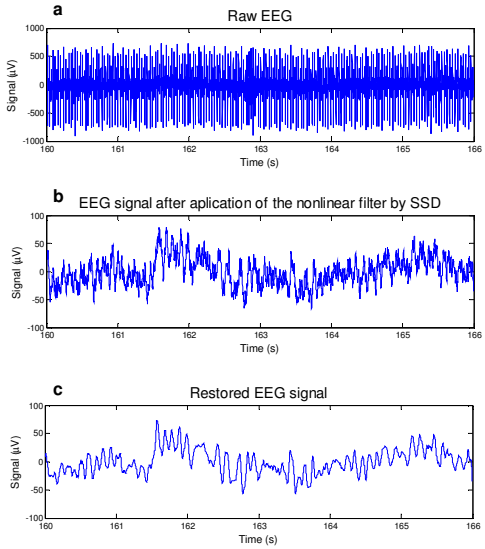


Fig. 3. Illustrative application of the proposed methodology for gradient artefact correction: (a) Typical raw EEG signal; (b) EEG after application of the nonlinear filter in the raw EEG; (c) restored EEG signal ($J = 200$).

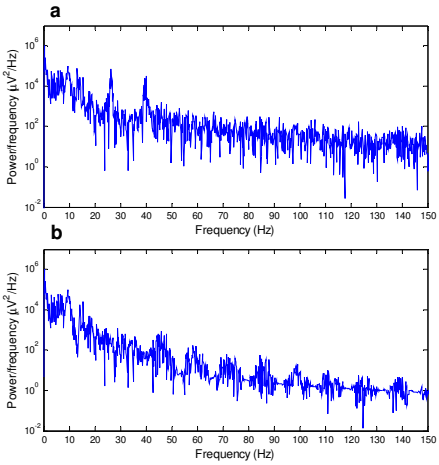


Fig. 4. Power spectrum of: (a) the nonlinear filtered signal; and (b) the restored EEG signal of Fig. 3.

effectively attenuated during application of the nonlinear filter by SSD as well, and are not observed in Figs. 3b and 3c. Fig. 5 depicts the $\mathbf{E\hat{E}G_{true}}$ and the respective partial waveform components ($J = 60$) resulting from the recursive application of the optimized moving-average filter in the $\mathbf{EEG_{corct}}$. Fig. 6 demonstrates the convergence of the limit described in (9), and how the maximum magnitude of the signal $\mathbf{EEG_{rest,\mathit{j}}}$ decreases with the increasing number of iterations, $j$. We noticed that at $J = 60$, the maximum magnitude of the signal $\mathbf{EEG_{rest,\mathit{j}}}$ reaches less than 0.5% of its value at the first iteration, whereas at $J = 200$, such magnitude is smaller than 0.1%. Considering the $\mathbf{EEG_{corct}}$, a large number of iterations results in a better estimation of the restored EEG. Nevertheless, we have experimentally observed that high-frequency components associated with the clinical EEG can be satisfactorily preserved

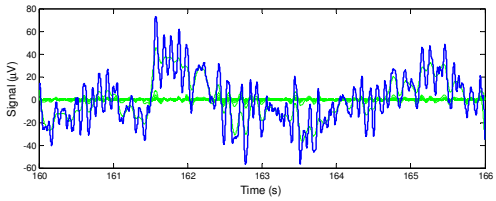


Fig. 5. Restored EEG signal (blue trace) and the respective partial waveform components $\mathbf{EEG}_{\mathbf{rest},j}$ (green traces) ($J = 60$).

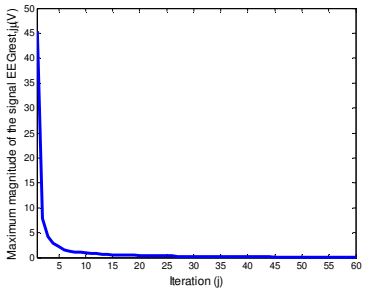


Fig. 6. Maximum magnitude of the signal $\mathbf{EEG}_{\mathbf{rest},j}$, according to the number of iterations performed by the optimized moving-average filter ($J = 60$).

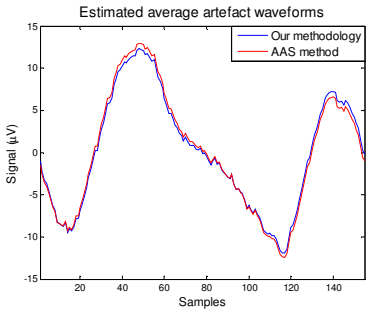


Fig. 7. Average artefact waveforms obtained by our proposed methodology (blue trace), and by the AAS method (red trace).

in the $\hat{\mathbf{EEG}}_{\mathbf{true}}$ for $J$ larger than 60 iterations. In Fig. 7, the estimated average artefact waveforms by our methodology ($J = 60$) and by the AAS method are depicted, considering the signal $\mathbf{EEG}_{\mathbf{corct}}$ of Fig. 3b (between 162.85 and 165.35 s), and a window length of 32 slices [17]. For estimation of such average waveforms, the $\mathbf{EEG}_{\mathbf{corct}}$ was segmented and interpolated in accordance with the implementation of the AAS methodology [4]. Such waveforms show to be quite similar, with mean standard deviation of the difference between them calculated at 0.4 μV, and median cross-correlation equal to 0.999, considering all validation channels and subjects. This fact demonstrates that the artefact estimative $\mathbf{A}_{\mathbf{artf}}$ does represent the gradient artefact interference, as predicted in (9). Since the gradient artefact activity calculated by our methodology does not constitute an artefact template, the variability of the artefact waveform over the time is predicted within the artefact estimative $\mathbf{A}_{\mathbf{artf}}$ as well. The power spectral difference was calculated in order to compare the median power spectrum of EEG excerpts with no fMRI, $S_{NF}$, with the median power spectrum of the restored EEG with fMRI, $S_F$ [4]:

$$\text{Difference} = 100 \times \text{absolute}\left(\frac{S_{NF} - S_F}{S_{NF}}\right)\% \qquad (12)$$

For calculation of the $S_{NF}$, the EEG excerpts with no fMRI were filtered by the nonlinear filter as well as by the optimized moving-average filter ($J = 60$), as performed for the restored EEG excerpts of the same channel. Considering EEG recordings from the 15 subjects and the EEG validation channels, the spectral power difference calculated within the frequency bands 0 – 4 Hz, 4 – 8 Hz, 8 –12 Hz, and 12 – 24 Hz, was 2.8%, 13.6%, 6.2%, and 8.6%, respectively. We have noticed that this difference decreases, as $J$ increases.

## IV. Discussion and Conclusions

Albeit a number of approaches have been proposed and achieved a satisfactory removal of gradient artefacts from the EEG signal recorded within the fMRI scanner, their improvement as well as the development of further correction techniques are still demanded in order to enhance the quality of the restored EEG [9, 12, 16]. In this sense, we have proposed a novel methodology to remove the artefact, which combines an optimized moving-average filtering approach with the nonlinear filtering method proposed in [25], as depicted in Fig. 1. Such nonlinear filter approach is used to attenuate the artefact activity before application of the optimized moving-average filter. In turn, the MA filter performs the restoration of the EEG signal by a recursive estimation either of the gradient artefact waveform along the entire EEG excerpt, which is subtracted afterwards (10); or alternatively, of partial waveforms partial components which compose the restored EEG (11). As shown in Figs. 2, 3, and 4, application of the methodology depicted in Fig. 1 results in an effective removal of the gradient artefact. In addition to smooth the signal, the optimized MA filter removes gradient artefact interference contained into the bins regions [8], as can be noticed in the approximated flat regions of the spectrum of Fig. 4b. On the other hand, the nonlinear filter by SSD carries out an adaptive attenuation of artefact frequency components along the entire signal bandwidth, according to the characteristics of the signal slope parameter [25] (Figs. 2, 3, and 4). In case of periodic fMRI acquisition, we have noticed that this property allows attenuating the frequency activity associated with the EPI volume repetition. For continuous fMRI acquisition, the optimized MA filter can be even directly applied in the raw EEG. Nevertheless, residual high-frequency activity associated with the slice repetition could remain in the restored EEG for larger values of $J$, which requires the usage of additional approaches for removing it. In this case scenario, application of the nonlinear filter with a higher *thrs* (2) associated with a larger $J$ might constitute an alternative to preserve EEG high-frequency components. Such characteristics shall be better evaluated in future work. Since estimation of the artefact interference is not based upon the subtraction of an artefact waveform model or template [4, 11, 13, 17], resulting subtraction residuals are negligible within application of our

method, which enables its use for correction of EEG signals with small amplitude. Another advantage of using the proposed approach is that there is no need for time-alignment between EEG and fMRI clocks as well as extensive data segmentation. Finally, the optimized moving-average combined with the nonlinear filter seems to be effective under the occurrence of abrupt subject head motions [14, 16], which shall be better evaluated in future work as well. As further suggestion for future work, the proposed methodology should be applied and assessed for EEG data acquired within other types of fMRI equipments.

## ACKNOWLEDGMENT

We are grateful to Saskia van Liempt, M.D., and Col. Eric Vermetten, M.D., Ph.D. from the University Medical Center/Central Military Hospital, Utrecht, for providing the data presented in this work. This work has been made possible by a grant from the European Union and Erasmus Mundus – EBW II Project, and by a grant from CNPq – Science without Borders Program.

## REFERENCES

[1] J. Belliveau et al., "Functional mapping of the human visual-cortex by magnetic resonance-imaging," Science, vol. 254, pp. 716–719, 1991.

[2] R. Goebel and F. Esposito, "The added value of EEG-fMRI in imaging neuroscience," in EEG-fMRI: Physiological Basis, Technique and Applications, C. Mulert, L. Limieux, Eds. Verlag, Berlin, Heidelberg: Springer, pp. 97-112, 2010.

[3] P. Allen, G. Polizzi, K. Krakow, D. Fish, and L. Lemieux, "Identification of EEG events in the MR scanner: the problem of pulse artefact and a method for its subtraction," NeuroImage, vol. 8, pp. 229-239, 1998.

[4] P. Allen, O. Josephs, and R. Turner, "A method for removing imaging artifact from continuous EEG recorded during functional MRI," NeuroImage, vol. 12, pp. 230-239, 2000.

[5] P. Ritter, R. Becker, F. Freyer, and A. Villringer, "EEG quality: the image acquisition artifact," in EEG-fMRI: Physiological Basis, Technique and Applications, C. Mulert, L. Limieux, Eds. Verlag, Berlin, Heidelberg: Springer, pp. 153-171, 2010.

[6] C. Mulert and U. Hegerl, "Integration of EEG and fMRI," in Neural Correlation of Thinking, E. Kraft, G. Gulyás, E. Pöppel, Eds. Verlag, Berlin, Heidelberg: Springer, pp. 95-106 , 2009.

[7] W. Olson, "Basic concepts of medical instrumentation," in Medical Instrumentation: Application and Design, J. Webster, Ed, 4th ed. New York: Wiley, pp. 1-44, 2010.

[8] R. Niazy, C. Beckmann, G. Iannetti, J. Brady, and S. Smith, "Removal of FMRI environment artifacts from EEG data using optimal basis sets," NeuroImage, vol. 28, pp. 720-737, 2005.

[9] K. Mullinger, W. Yan, and R. Bowtell, "Reducing the gradient artefact in simultaneous EEG-fMRI by adjusting the subject's axial position," NeuroImage, vol. 54, pp. 1942-1950, 2011.

[10] H. Mandelkow, P. Halder, P. Boesiger, and D. Brandeis, "Synchronization facilitates removal of MRI artefacts from concurrent EEG recordings and increases usable bandwidth," NeuroImage, vol. 32, pp. 1120-1126, 2006.

[11] S. Gonçalves, P. Pouwels, J. Kuijer, R. Heethaar, and J. De Munck, "Artifact removal in co-registered EEG/fMRI by selective average subtraction," Clin. Neurophysiol., vol. 118, pp. 823-838, 2007.

[12] J. De Munck, P. Van Houdt, S. Gonçalves, E. Van Wegen, and P. Ossenblok, "Novel artefact removal algorithms for co-registered EEG/fMRI based on selective averaging and subtraction," NeuroImage, vol. 64, pp. 407-415, 2013.

[13] M. Koskinen and N. Vartiainen, "Removal of imaging artifacts in EEG during simultaneous EEG/fMRI recording: reconstruction of a high-precision artifact template," NeuroImage, vol. 46, pp. 160-167, 2009.

[14] W. Yan, K. Mullinger, M. Brookes, and R. Bowtell, "Understanding gradient artefacts in simultaneous EEG/fMRI", NeuroImage, vol. 46, pp. 459-471, 2009.

[15] L. Sun and H. Hinrichs, "Simultaneously recorded EEG-fMRI: removal of gradient artifacts by subtraction of head movement related average artifact waveforms," Hum. Brain Mapp., vol. 30, pp. 3361–3377, 2009.

[16] M. Moosmann, V. Schönfelder, K. Specht, R. Scheeringa, H. Nordby, and K. Hugdahl, "Realignment parameter-informed artefact correction for simultaneous EEG-fMRI recordings," NeuroImage, vol. 45, pp. 1144-1150, 2009.

[17] J. Ferreira, P. Cluitmans, and R.M. Aarts, "Gradient artefact modelling using a set of sinusoidal waveforms for EEG correction during continuous fMRI," Signal Processing Research, vol. 2, pp. 39-48, 2013a.

[18] M. Negishi, M. Abildgaard, T. Nixon, and R. Constable, "Removal of time-varying gradient artifacts during continuous fMRI," Clin. Neurophysiol., vol. 115, pp. 2181-92, 2004.

[19] D. Mantini, M. Perucci, S. Cugini, G. Romani, and C. Del Gratta, "Complete artifact removal for EEG recorded during continuous fMRI using independent component analysis," NeuroImage, vol. 34, pp. 598-607, 2007.

[20] M. Brookes, K. Mullinger, C. Stevenson, P. Morris, and R. Bowtell, "Simultaneous EEG source localisation and artefact rejection during concurrent fMRI by means of spatial filtering," NeuroImage, vol. 40, pp. 1090-1104, 2008.

[21] A. Hoffmann, L. Jäger, K. Werhahn, M. Jaschke, S. Noachtar, and M. Reiser, "Electroencephalography during functional echo-planar imaging: detection of epileptic spikes using post-processing methods," Magn. Res. Med., vol. 44, pp. 791-798, 2000.

[22] J. Sijbers, I. Michiels, M. Verhoye, J. Van Auderkerke, A. Van der Linden, and D. Van Dyck, "Restoration of MR-induced artifacts in simultaneously recorded MR/EEG data," Magn. Res. Imaging., vol. 17, pp. 1383-1391, 1999.

[23] J. Sijbers, J. Van Audekerke, M. Verhoye, A. Van der Linden, and D. Van Dyck, "Reduction of ECG and gradient related artifacts in simultaneously recorded human EEG/fMRI data," Magn. Reson. Imaging., vol. 18, pp. 881-886, 2000.

[24] F. Grouiller, L. Vercueil, A. Krainik, C. Segebarth, P. Kahane, and O. David, "A comparative study of different artefact removal algorithms for EEG signals acquired during functional MRI," NeuroImage, vol. 38, pp. 124-137, 2007.

[25] J. Ferreira, P. Cluitmans, and R.M. Aarts, "Non-linear filter for gradient artefact correction during simultaneous EEG-fMRI," Signal Processing Research, vol. 2, pp. 55-63, 2013b.

[26] S. Van Liempt, E. Vermetten, E. Lentjes, J. Arends, and H. Westenberg, "Decreased nocturnal growth hormone secretion and sleep fragmentation in combat-related posttraumatic stress disorder; potential predictors of impaired memory consolidation," Psychoneuroendocrino., vol. 36, pp. 1361-1369, 2011.

[27] J. Ferreira, P. Cluitmans, and R.M. Aarts, "Gradient artefact correction in the EEG signal recorded within the fMRI scanner," in *Proc. 5th International Conference Bio-inspired Systems and Signal Processing,* Vilamoura, Portugal, pp. 110-117, 2012.

[28] G. Garreffa et al., "Real-time MR artifacts filtering during continuous EEG/fMRI acquisition," Magn. Res. Imaging., vol. 21, pp. 1175-1189, 2003.

[29] J. Ferreira, P. Cluitmans, and R.M. Aarts, "Detection of sharp wave activity in biological signals using differentiation between consecutive samples," in *Proc. 6th International Conference Bio-inspired Systems and Signal Processing,* Barcelona, Spain, pp. 327-332, 2013c.

[30] A. Oppenheim and R. Schafer, Discrete-Time Signal Processing, 2nd ed. New Jersey: Prentice-Hall, 1999.

[31] R. Rangayyan, Biomedical Signal Analysis: a Case-Study Approach. New York: Wiley, 2002.